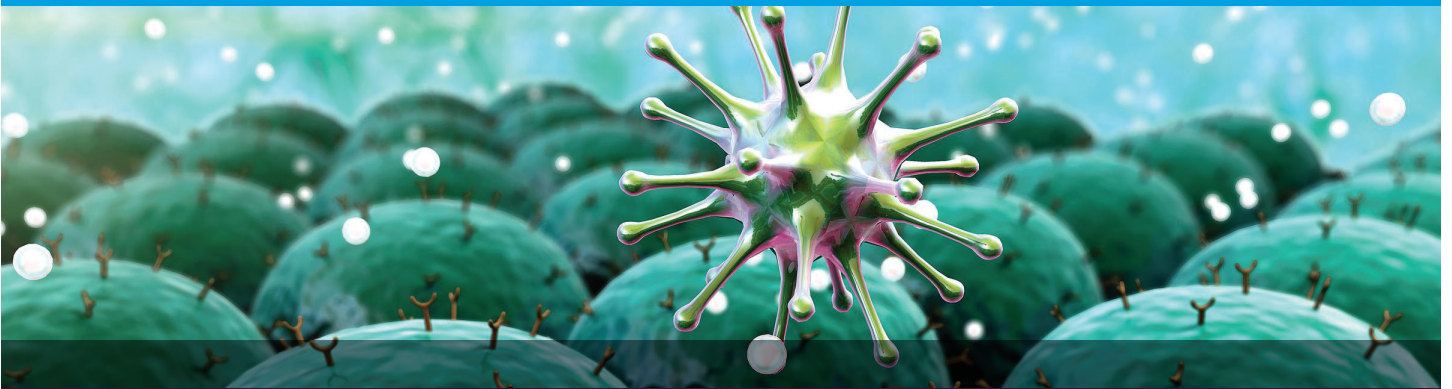# Infectious Disease Applications

Agilent xCELLigence RTCA handbook

# Table of Contents

# Overview

## Infectious disease assays in real time

The *in vitro* monitoring of host-pathogen interactions has a long history of being used for both clinical research and mechanistic studies. In both of these contexts, host-pathogen interactions can be analyzed at either the cellular or molecular levels. At the cellular level, pathogen-induced changes in the host cell can be monitored through different types of microscopy or colorimetric assays. A prime example of this is the cytopathic effect induced by viruses where infected host cells display rounding/swelling, detachment from the substrate, lysis, and other defining characteristics. The formation of inclusion bodies that are visible by microscopy, as occurs during the intracellular infection of fibroblasts by the *Chlamydia* bacterium, is another example. Alternatively, the live/dead status of pathogen-infected cells can be assessed through colorimetric assays using reagents such as MTT.

At the molecular level, host-pathogen interactions can be studied by monitoring diverse phenomena such as suppression of host DNA or mRNA synthesis, the rerouting of host proteins to different intracellular compartments, modification of chromatin structure, or altered phosphorylation patterns. The myriad techniques used for these molecular analyses include techniques from qPCR and flow cytometry to DNA sequencing and Western blotting.

A major shortcoming for the vast majority of the traditional cellular and molecular assays used for identifying, quantifying, and tracking infectious diseases in the clinic or research lab is that they are endpoint assays, providing only a snapshot of the infection process. As such, kinetic information is difficult or impossible to derive because one must often extrapolate or interpolate using a limited number of data points. Moreover, many of the traditional assays require labeling, which can reduce the assay's physiological relevance and is low-throughput and laborious. This means multiple sample handling steps are required that introduce variability. Accordingly, *in vitro* infectious disease studies would greatly benefit from a label-free assay that couples information-rich real-time kinetics with an easy workflow, high reproducibility, and high-throughput capabilities. This handbook describes how the xCELLigence real-time cell analysis (RTCA) systems deliver each of these attributes in the context of live cell assays. Example data from diverse bacterial, viral, and parasite applications are used to highlight the extreme utility of RTCA for infectious disease research applications.

## xCELLigence RTCA instruments

The nine different xCELLigence RTCA systems made by Agilent Technologies all use noninvasive biosensors monitoring cellular impedance (explained in the next section) to quantify cell proliferation, morphology change, cell-cell adhesion (that is, barrier function), and cell-substrate attachment quality in a label-free and real-time manner. The four xCELLigence instruments that are best suited for infectious disease research are shown in the following table. Their plate format/throughput differs, and some of the instruments possess specialized functionalities, such as the ability to monitor cell invasion/migration.



|  | Dual Purpose (DP) | Single Plate (SP) | Multiple Plates (MP) | High Throughput (HT) | eSight |
|---|---|---|---|---|---|
| Format | 3 × 16 wells | 1 × 96 wells | 6 × 96 wells | 1 × 384 wells | 3 × 96 wells impedance, 5 × 96 wells imaging |
| Maximum throughput | 48 wells | 96 wells | 576 wells | Up to 4 × 382 wells (1,536 wells total) | 288 wells impedance, up to 480 wells total for imaging |

xCELLigence RTCA instruments are typically housed inside a standard $CO_2$ cell culture incubator or hypoxia chamber and controlled by a computer that sits outside the incubator (Figure 1). Intuitive software enables real-time interfacing with the instrument and includes data display and analysis functions.



**Figure 1.** Example of an Agilent xCELLigence instrument. The instrument is placed inside a standard tissue culture incubator, and is compatible with the full range of biologically relevant temperatures, atmospheric compositions, and humidities. The instrument is controlled by a laptop computer stationed outside the incubator.

## Cellular impedance

The functional unit of the xCELLigence impedance assay is a set of gold biosensors embedded in the bottom surface of a microplate well (Figure 2). When submersed in an electrically conductive solution (such as buffer or standard tissue culture medium), the application of a weak electric potential across these biosensors causes an electric current to flow between them. Because this phenomenon is dependent on the biosensors interacting with bulk solution, the presence of adherent cells at the biosensor-solution interface impedes the electrical current flow. The magnitude of this impedance depends on the number of cells, the size of the cells, cell-cell adhesion (barrier function), and the cell-substrate attachment quality. Neither the gold biosensor surfaces nor the applied electric current has an effect on cell health or behavior.
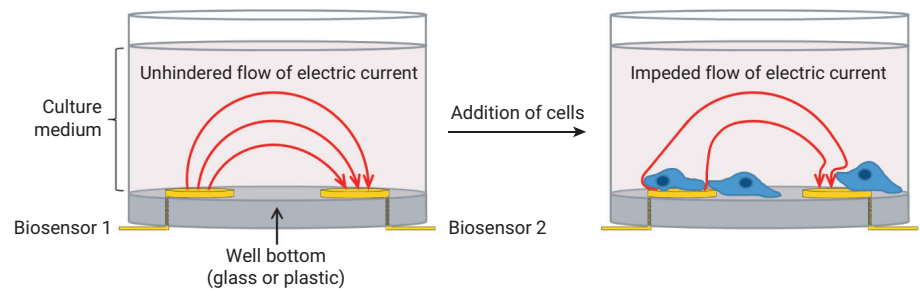


**Figure 2.** Overview of a cellular impedance apparatus. A side view of a single well is shown before and after cells have been added. Neither the biosensors nor the cells are drawn to scale (they have been enlarged for clarity). In the absence of cells, electric current flows freely through culture medium, completing the circuit between the biosensors. As cells adhere to and proliferate on the biosensors, current flow is impeded, providing an extremely sensitive readout of multiple parameters.

## E-Plates

The gold biosensors in each well of Agilent electronic microplates (E-Plates) cover ~75% of the bottom surface area. Figure 2 depicts a simplified presentation of the biosensor. A more detailed depiction in Figure 3 shows the circular biosenors are linked into strands that form an interdigitating array. This proprietary design enables large populations of cells to be monitored simultaneously, and provides exquisite sensitivity to changes in cell number, size, and attachment strength.
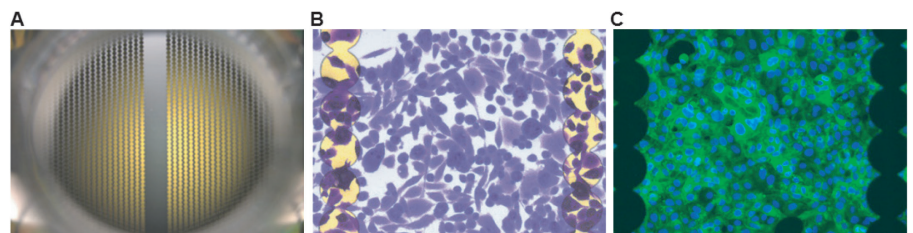


**Figure 3.** Impedance biosensors in Agilent E-Plates. (A) Photograph of a single well in an E-Plate. Though cells can also be visualized on the gold electrode surfaces, the electrode-free region in the middle of the well facilitates microscopic imaging. (B) Gold biosensors and crystal violet-stained human cells, as viewed in a reflected light microscope. (C) Immunofluorescence microscopy with gold biosensors silhouetted.

## Real-time impedance traces explained

The impedance of electric current caused by adherent cells is reported using a unitless parameter called Cell Index (CI), where:

$$CI = \frac{(\text{Impedance at n}) - (\text{Impedance without cells})}{(\text{nominal impedance constant})}$$

Figure 4 provides a generic example of a real-time impedance trace throughout the course of setting up and running an apoptosis experiment. For the first few hours after cells have been added to a well, there is a rapid increase in impedance, which is caused by cell attachment and spreading. If cells are subconfluent after the initial attachment stage, they will start to proliferate, causing a gradual, yet steady increase in CI. When cells reach confluence, the CI value plateaus, reflecting that the electrode surface area accessible to bulk media is no longer changing. The addition of an apoptosis inducer at this point, such as a bacterial toxin, causes a decrease in CI down to zero. This is the result of cells rounding then detaching from the well bottom. While this example involves addition of the apoptosis inducer at the point of cellular confluence, impedance-based assays are extremely flexible, and can interrogate a wide variety of phenomena across the full spectrum of cell densities.
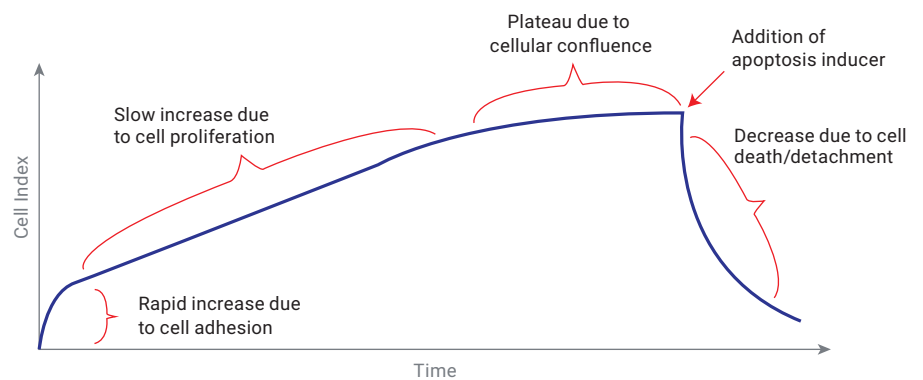


**Figure 4.** Generic real-time impedance trace for setting up and running an apoptosis assay. Each phase of the impedance trace, and the cellular behavior it arises from, is explained in the text.

## Broad adoption of xCELLigence RTCA

More than 2,000 xCELLigence instruments have been placed in labs that span academia, biotech, and contract research organizations. This has resulted in >1,400 xCELLigence publications in peer-reviewed journals (Figure 5). A large and growing percentage of these papers are focused on infectious diseases.
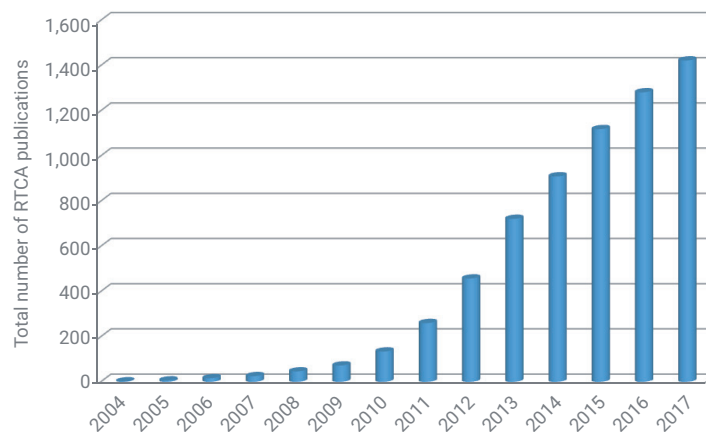


**Figure 5.** Total number of xCELLigence RTCA publications as a function of time.

# Bacteria: detection and quantification of secreted toxins

RTCA excels at monitoring the dynamic changes in cell number, morphology, and adhesion strength that are induced in host cells as they interact with bacterial toxins. RTCA has been used extensively to monitor dynamic changes with *Vibrio cholerae* toxin,[1] *Clostridium botulinum* toxin,[2] and *Clostridium difficile* toxin,[3,4] as described below.

*C. difficile* is recognized as a significant nosocomial and community-acquired pathogen, leading to infectious diarrhea that develops after hospitalization or receiving antibiotic treatment. Because *C. difficile* protein toxins A and B are the key determinants of virulence, a definitive diagnosis of *C. difficile* infection (CDI) requires detection of either these proteins or the genes that encode them.

Historically, the gold standard for *C. difficile* diagnosis has been a cytotoxigenic assay wherein stool samples are incubated *in vitro*, then tested for the presence of protein toxin by monitoring the sample's effect on cultured human cells.[5] Although this cytotoxigenic assay is informative, it is not widely used in clinical research settings because it is labor intensive, subjective, and time consuming. As alternatives, several enzyme immunoassays (EIAs) and PCR-based toxin gene detection assays approved by the Food and Drug Administration are routinely used in clinical laboratories.[6] However, these suffer from the following drawbacks: EIAs have low sensitivity, and the correlation between toxin gene detection by PCR and disease onset is a matter of debate. Moreover, highly sensitive PCR-based assays can lead to overdiagnosis of CDI and unnecessary therapy because they do not distinguish *bona fide C. difficile* infection from mere colonization.[7] Taken together, CDI diagnosis clearly remains controversial. A rapid and objective assay with an easy workflow is needed.

Multiple groups reported using RTCA for the quantitative detection of *C. difficile* toxin.[4–6] In one of these studies, Hs27 fibroblast cells were exposed to different concentrations of purified *C. difficile* toxin B4. As shown in Figure 6A, after allowing the cells to grow to the point of confluence, evidenced by the impedance signal plateaued, purified toxin was added and its effects were monitored as a time- and dose-dependent decrease in the CI (which correlates with toxin-induced cell death and detachment). This assay was readily able to detect *C. difficile* toxin B at concentrations as low as 0.05 ng/mL, and displayed no cross-reactivity with other enterotoxins, nontoxigenic *C. difficile*, or other *Clostridium* species (data not shown here). To develop a standard curve that could be used for determining the concentration of *C. difficile* toxin B in clinical research samples, the time required for the normalized CI to drop to 50% of its initial value (the value immediately before toxin treatment) was plotted as a function of the toxin concentration to generate the curve shown in Figure 6B.
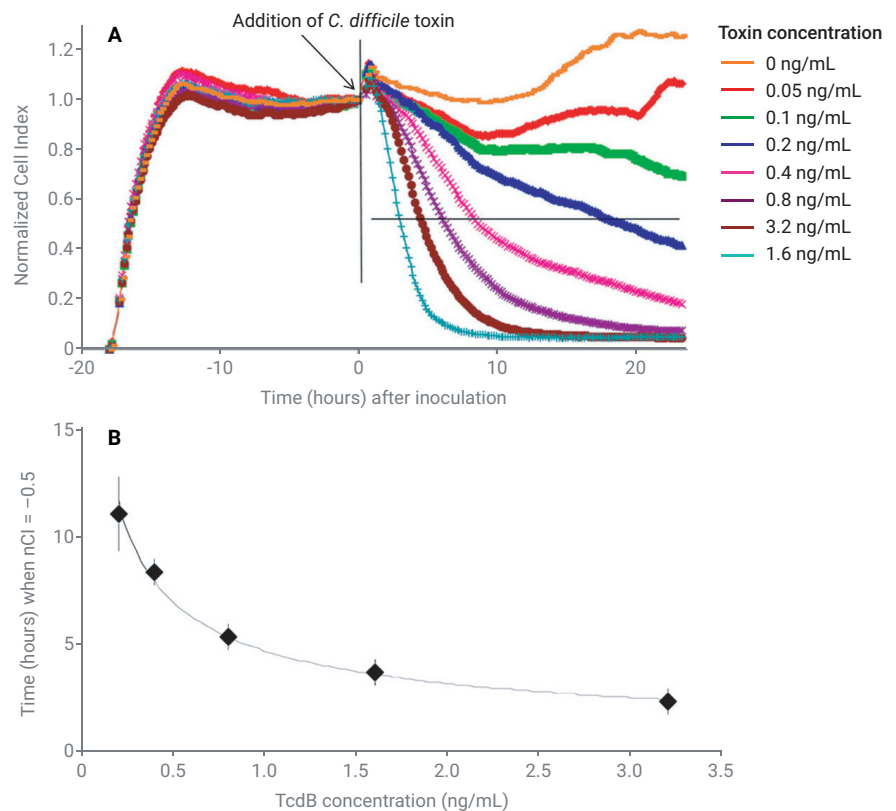


**Figure 6.** Quantitative detection of *C. difficile* toxin B using an Agilent xCELLigence RTCA instrument. (A) Hs27 cells (5,000 cells/well) were cultivated in Agilent E-plate wells, and cell attachment and spreading were monitored in real time for 17.5 hours before the addition of purified *C. difficile* toxin B at different concentrations. The cytotoxic effect was then monitored continuously for the next ~24 hours. The black vertical line denotes the time of toxin addition (t = 0). The bold horizontal line in the middle of the plot represents a 50% decrease in CI, relative to its starting value (that is, immediately before toxin addition). This is referred to as the normalized CI 50% value, or nCI = 0.5. As expected, the time required for reaching nCI=0.5 is dependent on the concentration of the toxin. (B) By plotting nCI = 0.5 as a function of toxin concentration, a standard curve was developed, which can be used for determining the concentration of toxin in clinical research samples.

Figure adapted from the *Journal of Clinical Microbiology*, volume *48*, Ryder, A. B. *et al.* "Clostridium difficile Infections by Quantitative Detection of tcdB Toxin by Use of a Real-Time Cell Analysis System," pages 4129–4134. Copyright **2010**, with permission from the American Society for Microbiology.

Validation of the RTCA *C. difficile* toxin assay was performed using 300 stool specimens with suspected *C. difficile* infection. A sample was scored as being positive or negative for *C. difficile* toxin depending on whether or not it caused a time-dependent drop in normalized CI that could be rescued by the addition of a toxin-specific neutralizing antibody (Figure 7). This RTCA-based scoring approach showed strong correlation with standard cytotoxicity detection using immunohistochemistry/microscopy (Figure 7).
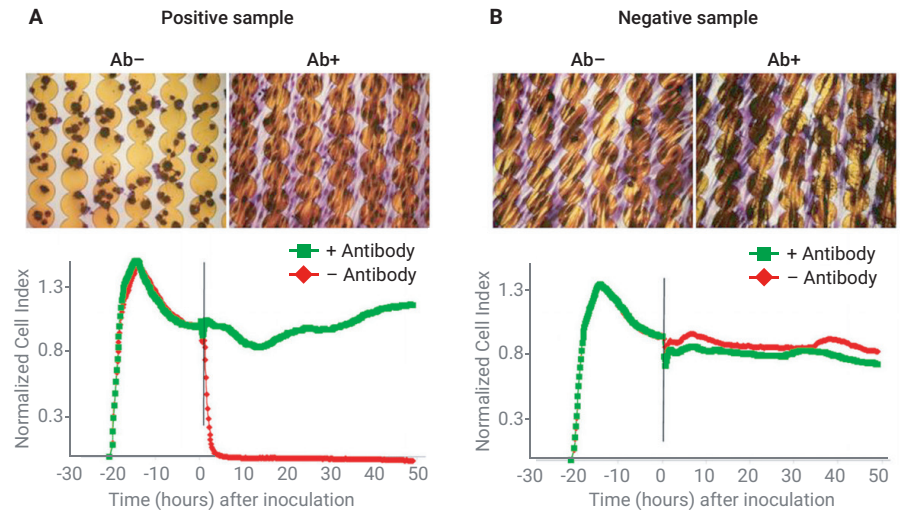


**Figure 7.** Testing for the presence of *C. difficile* toxin in stool samples from infected and uninfected subjects. The RTCA assay described in the text was performed in parallel with a conventional cytotoxicity assay wherein cells were stained and analyzed by microscopy directly in Agilent E-Plate wells. The cytotoxic effect is readily visible in the positive sample when using either microscopy or the RTCA assay. As expected, the addition of neutralizing antibody abolishes the cytotoxic effect of *C. difficile* toxin present in the positive sample, but has no impact on the negative sample from an uninfected subject.

Using *C. difficile* toxin B as an example, the above study demonstrates that RTCA is an effective tool for applications involving bacterial toxins. Through the use of a standard curve and a neutralizing antibody, RTCA can be used in a clinical research setting to confirm the presence of a bacterial toxin, determine the toxin's concentration, and monitor the efficacy of therapeutic intervention over time. Beyond the clinic, the sensitivity of RTCA to dynamic changes in cell health and behavior can be used for various research applications, such as identifying a binding target of a bacterial toxin on the host cell surface, and comparing antitoxin efficacies.

## References—RTCA for studying bacterial toxins (not exhaustive)

## References—General

1. Jin, D. *et al.* Quantitative Detection of *Vibrio cholerae* Toxin by Real-Time And Dynamic Cytotoxicity Monitoring. *J. Clin. Microbiol.* **2013** Dec, *51(12)*, 3968−74.

2. Real-Time Cell-Based Toxicology Testing Might Replace Animal Testing for Product Release and Drug Safety. *Biochemica* **2008**, 11−13.

3. Ryder, A. B. *et al.* Assessment of *Clostridium difficile* Infections by Quantitative Detection of tcdB Toxin by Use of a Real-Time Cell Analysis System. *J. Clin. Microbiol.* **2010**, *48*, 4129−4134.

4. Huang, B. *et al.* Real-Time Cellular Analysis Coupled with a Specimen Enrichment Accurately Detects and Quantifies *Clostridium difficile* Toxins in Stool. *J. Clin. Microbiol.* **2014**, *52*, 1105−1111.

5. Pollock, N. R. Ultrasensitive Detection and Quantification of Toxins for Optimized Diagnosis of *Clostridium difficile* Infection. *J. Clin. Microbiol.* **2016**, *54*, 259−264.

6. Planche, T. *et al.* Diagnosis of *Clostridium difficile* Infection by Toxin Detection Kits: A Systematic Review. *Lancet Infect. Dis.* **2008**, *8*, 777−784.

7. Polage, C. R. *et al.* Overdiagnosis of *Clostridium difficile* Infection in the Molecular Test Era. *JAMA Intern. Med.* **2015**, *175*, 1792−1801.

# Bacteria: host cell interactions

In contrast to the secreted protein toxins described in the previous section, some bacteria spread disease through direct interaction with, or invasion of, host cells. These interactions typically result in changes to the host cell, which can be detected through RTCA monitoring.

*Neisseria meningitidis* is the Gram-negative bacterium that causes meningitis, a disease that results in developmental impairment or death in approximately 10% of infected children. Once inside the blood stream, *N. meningitidis* uses type IV pili to bind the apical surface of brain endothelial cells. This interaction induces activation of signaling pathways within the host cell, gross morphological changes, and the breakdown of intercellular junctions with neighboring cells. Collectively, these changes are what enable the bacterium to extravasate from brain capillaries and infect the meninges (the protective lining of the central nervous system).[1]

Slanina and coworkers developed an xCELLigence assay to study the key virulence determinant of *N. menigitidis* in real time. The assay used a confluent monolayer of human brain microvascular endothelial cells (HBMECs) exposed to isogenic strains of the bacterium.[2] When MC58 (an isolate of infectious *N. meningitidis*) was added, the impedance signal displayed a transient increase followed by a rapid drop to a value of nearly zero (Figure 8A). This drop in the impedance signal correlated with: (1) HBMEC membrane disruption, as evidenced by the release of matrix metalloproteinase 8 (MMP-8) into the medium (Figure 8B), and (2) detachment of the HBMEC from the plate bottom (Figures 8B and 8C). To assess the importance of the bacterium's capsule in effecting this change, MC58 was compared with an *siaD* isogenic mutant, which is deficient for capsule production. The importance of the *N. meningitidis* lipopolysaccharide (LPS) and OPC membrane protein were also evaluated using isogenic mutants. As seen in Figures 8D–8F, the bacterial capsule and LPS had an impact on the kinetics but not to the same extent as the bacterium's cytopathic effect. OPC was inconsequential in this particular assay.
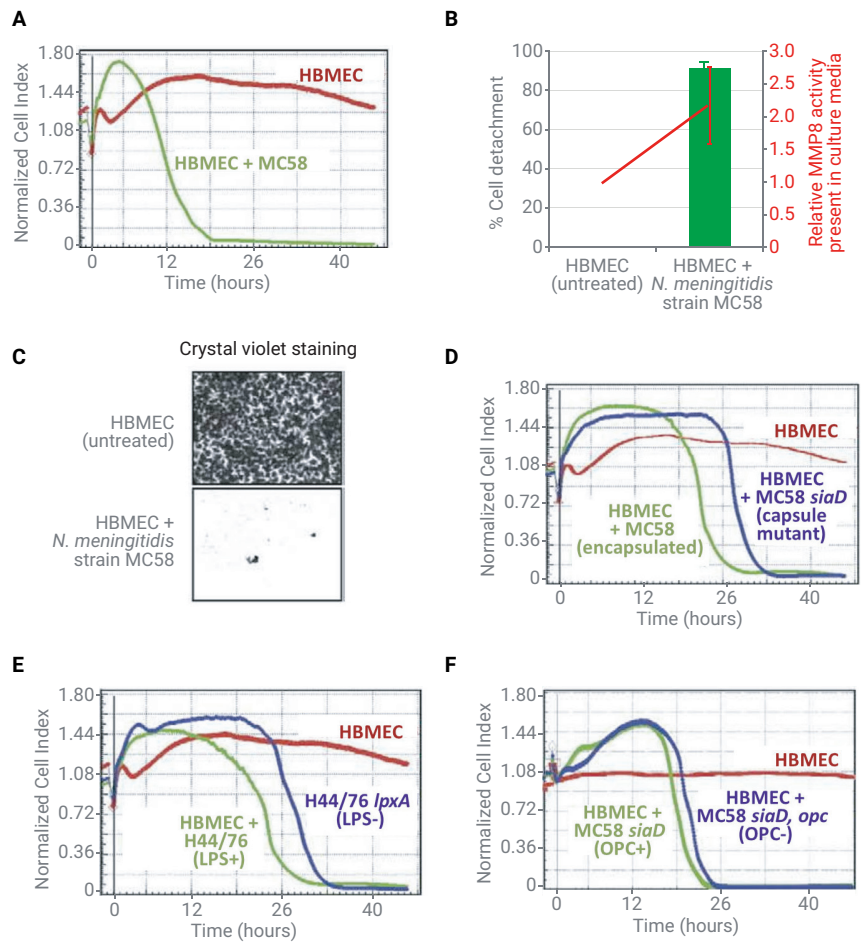
**Figure 8.** Identifying key virulence factors during *N. meningitidis* infection of HBMECs. (A) Infection of HBMECs with the MC58 strain of *N. meningitidis* causes a rapid loss in the HBMEC impedance signal, consistent with a cytotoxic effect. (B) The drop in impedance signal correlates with target cell detachment and membrane disruption, releasing MMP8 into the culture medium (MMP8 activity was detected through cleavage of a fluorescent substrate). (C) Crystal violet staining showing detachment of HBMECs after treatment with MC58. (D,E) Comparison of isogenic strains demonstrating that deficiencies in the *N. meningitidis* capsule or LPS slow the cytopathic effect, but do not impact the overall extent of HBMEC killing/lysis. (F) Loss of the membrane protein OPC has minimal impact on the cytopathogenicity of *N. meningitidis*.

Reprinted from the *Journal of Microbiological Methods*, volume *84 (1)*, Slaninak, H. *et al.* "Real-Time Impedance Analysis of Host Cell Response to Meningococcal Infection," pages 101–8. Copyright **2011**, with permission from Elsevier.

Another noteworthy example of xCELLigence RTCA being used to study bacteria-host interactions involves *Salmonella typhimurium*, the causative agent of typhoid. When binding to a human intestinal epithelial cell, *S. typhimurium* injects the host cell with bacterial proteins that cause cytoskeletal rearrangements. This process culminates in the host cell's membrane ruffling/protruding outward, and the engulfment of the bacterium within an endocytic vacuole. Inside the vacuole, *S. typhimurium* suppresses normal degradation through fusion with lysosomes, and turns the vacuole into a bacterial replication compartment.

When Mou and colleagues infected human epithelial HT-29 cells with *S. typhimurium*, the host cell-derived impedance signal displayed two distinct peaks, followed by a steady decrease (Figure 9A).[3] Using immunofluorescence microscopy, the first bacterium-induced peak (labeled as phase of infection "b" in Figure 9A) was found to correlate with membrane ruffling and the deposition of actin stress fibers at the site where the bacterium entered the host cell (Figure 9B). When the HT-29 cells were pretreated with the actin polymerization inhibitor cytochalasin D for 90 minutes before infection with *S. typhimurium*, this first impedance peak was abolished (Figure 9C). Using similar approaches, Mou *et al.* were able to assign distinct molecular/cellular phenomena to different phases of the impedance trace during *S. typhimurium* infection.
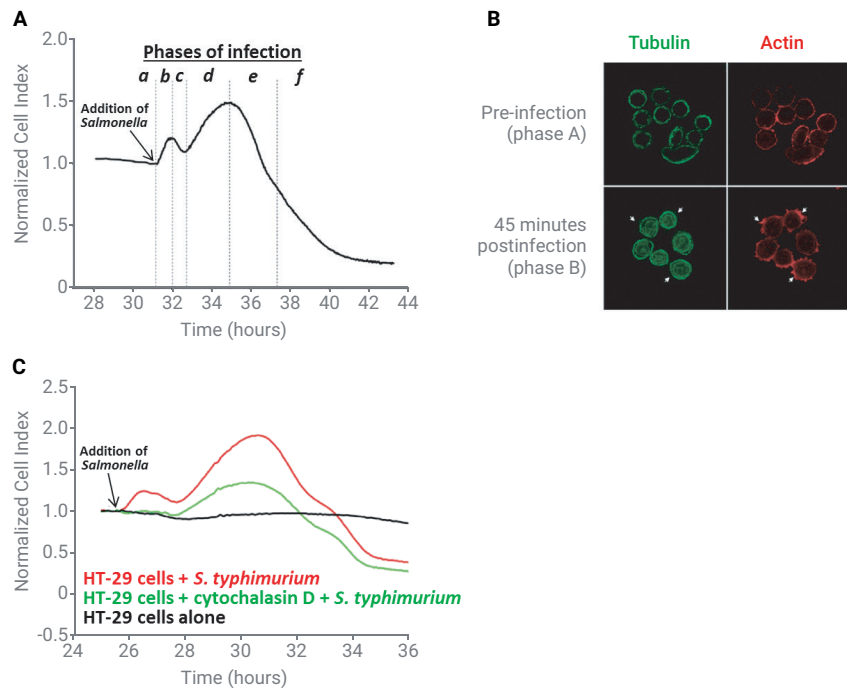


**Figure 9.** *S. typhimurium* infection of human intestinal HT-29 cells. (A) Immediately after encountering the bacterial cells, HT-29 cells display two spikes in their impedance signal, followed by a steady decrease. Distinct phases of this impedance response have been labeled with letters. (B) Immunofluorescent analysis of uninfected and infected HT-29 cells 45 minutes postinfection with *S. typhimurium*. Bacterial infection causes tubulin reorganization throughout the host cell, while actin stress fibers accumulate in the immediate vicinity of bacterial entry sites (denoted by white arrows). (C) Treating HT-29 cells with the potent actin polymerization inhibitor cytochalasin D for 90 minutes before *S. typhimurium* infection eliminates the first impedance peak, helping to provide a molecular explanation for the cause of this peak.

Figure adapted from *Public Library of Science One*, volume *6 (11)*, Mou, X. *et al.* "Phenotypic Pattern-Based Assay for Dynamically Monitoring Host Cellular Responses to Salmonella Infections." **2011**. This work is licensed under the Creative Commons Attribution 4.0 International License. To view a copy of this license, visit http://creativecommons.org/licenses/by/4.0/ or send a letter to Creative Commons, PO Box 1866, Mountain View, CA 94042, USA.

The study in Figure 9 highlights the wealth of information contained within real-time impedance traces. It also demonstrates the ease with which distinct features of the trace can be correlated with specific molecular or cellular phenomena. xCELLigence RTCA enables these phenomena to be studied in a continuous manner, to reveal mechanistic subtleties that would be difficult to piece together using endpoint data alone. This type of information can be used for many purposes, such as elucidating in which phase of infection a particular gene or protein plays a role or screening for drugs that disrupt a distinct step of the infection process.

References—general

References—RTCA for studying bacteria-host interactions (not exhaustive)

1. Coureuil, M. *et al.* Mechanism of Meningeal Invasion by *Neisseria meningitidis*. *Virulence* **2012**, Mar-Apr, *3(2)*, 164–72.

2. Slanina, H. *et al.* Real-Time Impedance Analysis of Host Cell Response to Meningococcal Infection. *J. Microbiol. Methods* **2011** Jan, *84(1)*, 101–8.

3. Mou, X. *et al.* Phenotypic Pattern-Based Assay for Dynamically Monitoring Host Cellular Responses to *Salmonella* Infections. *PLoS One* **2011**, *6(11)*, e26544.

4. Miranda-CasoLuengo, A. A. *et al.* A Real-Time Impedance Based Method to Assess *Rhodococcus equi* Virulence. *PLoS One* **2013**, *8(3)*, e60612.

5. Hidalgo-Cantabrana, C. *et al.* Effect of Bacteria Used in Food Industry on the Proliferation and Cytokine Production of Epithelial Intestinal Cellular Lines. *J. Functional Foods* **2014**, *6*, 348–355.

# Bacteria: biofilms

In addition to living in a free-floating planktonic state within aqueous environments, bacteria can also colonize biotic and abiotic surfaces at liquid-solid and air-solid interfaces. Within these microenvironments, secreted chemical messengers are used to coordinate gene expression profiles across the colony, thereby promoting survival. A common adaptation of these communities is the secretion of extracellular polymeric substances (EPS), which encapsulate the bacterial cells and protect them from the environment. The ability to form these biofilms is a key virulence factor because the EPS matrix facilitates bacterial evasion of host immune responses and also enhances the antibiotic resistance of bacteria as much as 1,000-fold.

In addition to playing critical roles in human dental plaque and cavities, chronic infections, rejection of artificial implants, and food poisoning, bacterial biofilms are also responsible for a large percentage of livestock diseases and cause fouling of industrial air and water handling systems, further increasing their economic impact. Though developing drugs to treat biofilms or prevent their formation is of critical importance, the colorimetric assays traditionally used for studying biofilms are inefficient or low-throughput, incompatible with orthogonal assays (samples are destroyed by the analysis process), and only provide endpoint data. Multiple research groups have recently described how impedance monitoring by xCELLigence RTCA instruments overcomes each of these limitations, enabling a quantitative and continuous evaluation of biofilms using an assay that is label free and totally automated.

As a first step towards understanding xCELLigence RTCA's capability to monitor biofilms, Alex Mira and colleagues demonstrated that both bacterial cells and EPS contribute to the impedance signal (data not shown here). They assessed the ability of RTCA to screen for biofilm-blocking agents (prophylactic activity) by including antibiotics in the growth media at the time that *S. aureus* 240 was seeded into E-Plate wells. Cells were allowed to grow for 20 hours, when the CI was compared to an untreated control.

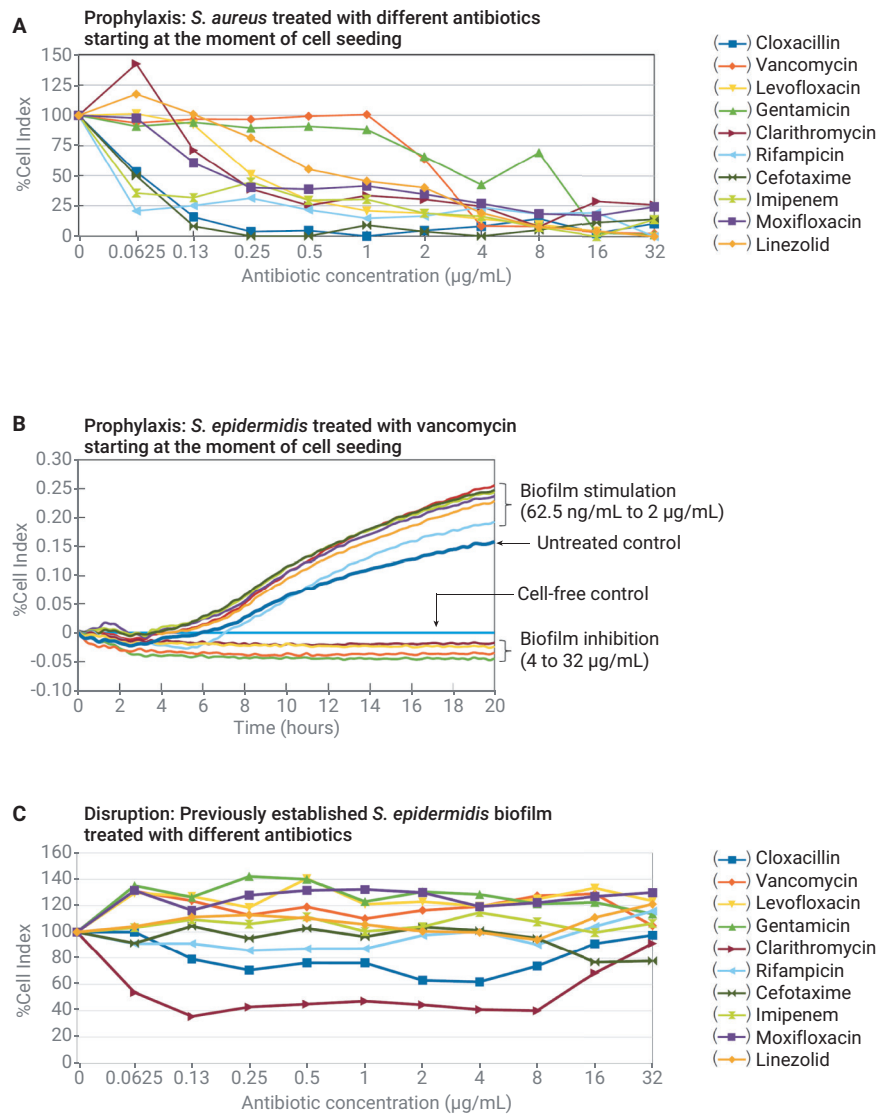In Figure 10A, the %Cell Index is defined as:

$$\frac{(\text{Cell Index})_{\text{with drug}}}{(\text{Cell Index})_{\text{without drug}}} \times 100$$

This is plotted as a function of drug concentration for 10 different drugs. Though each of the 10 antibiotics tested displayed prophylactic activity, they did this with differing levels of efficacy. While cefotaxime completely destroyed the biofilm-associated signal at a concentration of 0.25 µg/mL, linezolid required a 128-fold higher concentration to accomplish this (Figure 10A). This experiment demonstrated the utility of RTCA as a tool for drug screens aimed at preventing biofilms from forming.

Within particular concentration ranges, some antibiotics can actually promote biofilm growth. Being able to characterize this unwanted behavior is critical for preventing physicians from exacerbating the very infection they are trying to treat. This bifurcated behavior is readily detectable, and quantifiable, using RTCA. At concentrations of 4 to 32 µg/mL, vancomycin is found to suppress *S. epidermidis* 43040 biofilm growth, but at concentrations of 62.5 ng/mL to 2 µg/mL, biofilm growth is stimulated (Figure 10B).

Biofilm-disrupting activity was probed by allowing a biofilm of *S. epidermidis* 43040 to become established, and subsequently treating it with antibiotics. Figure 10C shows that at concentrations of 0.125 to 8 µg/mL, cloxicillin and rifampicin were able to induce partial disruption of the biofilm, with the CI dropping by ~60% in the most extreme case. The inability of the 10 tested antibiotics to cause complete biofilm disruption is consistent with the known antibiotic resistance of biofilms, demonstrates the importance of testing drug efficacy against the biofilm (rather than planktonic) state, and highlights the need for more effective drugs.

These experiments demonstrate the utility of xCELLigence RTCA for studying bacterial biofilms. The protocol involves substantially less work than traditional assays; bacteria are simply seeded into an E-Plate, after which data acquisition is continuous and automatic. The real-time nature of the xCELLigence data enables quantitative comparisons between different strains and treatments and allows evaluation of bacterial cells and their EPS. Achieving such a detailed and nuanced picture of biofilm dynamics using traditional endpoint assays would be costly in terms of staff hours and not provide the same level of reproducibility.

**A** Prophylaxis: *S. aureus* treated with different antibiotics starting at the moment of cell seeding

Legend:
- Cloxacillin
- Vancomycin
- Levofloxacin
- Gentamicin
- Clarithromycin
- Rifampicin
- Cefotaxime
- Imipenem
- Moxifloxacin
- Linezolid

**B** Prophylaxis: *S. epidermidis* treated with vancomycin starting at the moment of cell seeding

Biofilm stimulation (62.5 ng/mL to 2 µg/mL)
Untreated control
Cell-free control
Biofilm inhibition (4 to 32 µg/mL)

**C** Disruption: Previously established *S. epidermidis* biofilm treated with different antibiotics

Legend:
- Cloxacillin
- Vancomycin
- Levofloxacin
- Gentamicin
- Clarithromycin
- Rifampicin
- Cefotaxime
- Imipenem
- Moxifloxacin
- Linezolid

**Figure 10.** Using RTCA to screen for drugs that either prevent biofilm formation or disrupt established biofilms. (A) Ten different antibiotics (each represented by a different colored line) were evaluated for their ability to prevent *S. aureus* 240 from forming biofilm. Antibiotics were present at different concentrations from the moment bacteria were seeded into wells. 20 hours after seeding, the CI was measured and compared to the untreated control. The %Cell Index plotted here is.

$$\frac{(Cell\ Index)_{with\ drug}}{(Cell\ Index)_{without\ drug}} \times 100$$

(B) Testing for prophylactic activity. Depending on its concentration, vancomycin either inhibits or stimulates the growth of *S. epidermidis* 43040 biofilm. (C) Testing for biofilm disruption activity. At concentrations above 0.13 µg/mL, only cloxacillin and rifampicin are able to induce partial distruption of the *S. epidermidis* biofilm. %CI is defined above.
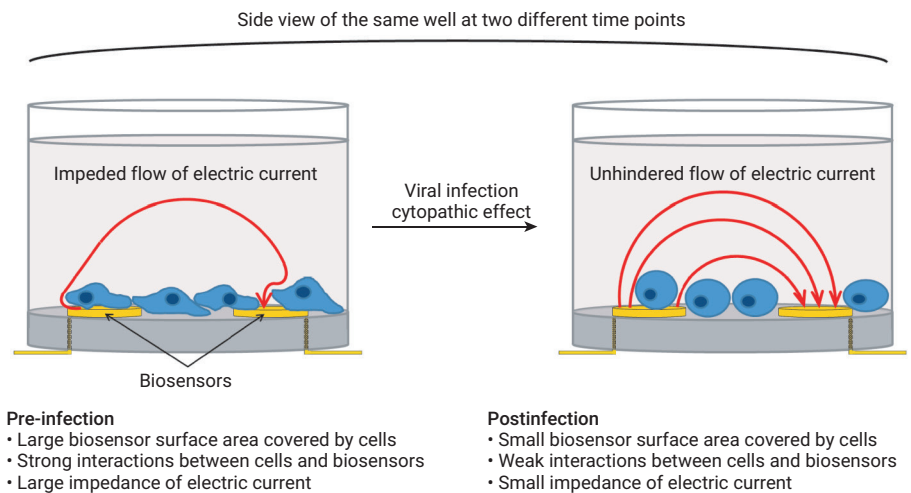
References—RTCA for studying biofilms

1. Junka, A. F. *et al.* Use of the Real Time xCelligence System for Purposes of Medical Microbiology. *Polish Journal of Microbiol.* **2012**, *61(3)*, 191–197.

2. Cihalova, K. *et al. Staphylococcus aureus* and MRSA Growth and Biofilm Formation after Treatment with Antibiotics and SeNPs. *Int. J. Mol. Sci.* **2015** Oct 16, *16(10)*, 24656–72.

3. Gutiérrez. D. *et al.* Monitoring in Real Time the Formation and Removal of Biofilms from Clinical Related Pathogens Using an Impedance-Based Technology. *PLoS One* **2016**, Oct 3, *11(10)*, e0163966.

4. Ferrer, M. D. *et al.* Effect of Antibiotics on Biofilm Inhibition and Induction measured by Real-Time Cell Analysis. *J. Appl. Microbiol.* **2016** Dec 8.

5. Wang, T.; Su, J. *Bacillus subtilis* from Soybean Food Shows Antimicrobial Activity for Multidrug-Resistant *Acinetobacter baumannii* by Affecting the adeS Gene. *J. Microbiol. Biotechnol.* **2016** Dec 28, *26(12)*, 2043–2050.

6. van Duuren, J. B. J. H. *et al.* Use of Single-Frequency Impedance Spectroscopy to Characterize the Growth Dynamics of Biofilm Formation in *Pseudomonas aeruginosa*. *Sci. Rep.* **2017** Jul 12, *7(1)*, 5223.

7. Gutiérrez, D. *et al.* Real-Time Assessment of *Staphylococcus aureus* Biofilm Disruption by Phage-Derived Proteins. *Front Microbiol.* **2017** Aug 24, *8*, 1632.

# Viruses: titer determination

When infected with a virus, host cells often display microscopically visible changes that are collectively referred to as a cytopathic effect (CPE). CPEs can include cell shrinkage or enlargement, deterioration, cell fusion, and the formation of inclusion bodies. Not all viruses cause a CPE in their host cell, but when they do it can be a useful tool for many research applications. In a typical CPE assay, a monolayer of cells is inoculated with a virus specimen, then monitored over days (or even weeks) to track morphological changes that emerge in distinct foci corresponding to sites of infection. This type of analysis are laborious and prone to variation due to the subjectivity of identifying and grading CPE foci. As a more efficient, objective, accurate, and higher throughput alternative, many labs have used xCELLigence RTCA to track viral CPEs for applications such as titer determination, neutralizing antibody analyses. The principle of tracking viral CPEs using impedance is illustrated in Figure 11.

Side view of the same well at two different time points

Impeded flow of electric current

Viral infection cytopathic effect

Unhindered flow of electric current

Biosensors

**Pre-infection**
• Large biosensor surface area covered by cells
• Strong interactions between cells and biosensors
• Large impedance of electric current

**Postinfection**
• Small biosensor surface area covered by cells
• Weak interactions between cells and biosensors
• Small impedance of electric current

**Figure 11.** Tracking viral CPEs using Agilent xCELLigence RTCA. Within Agilent E-Plates, virus-induced changes in host cell morphology and attachment strength (hallmarks of a cytopathic effect) are readily detected by changes in the ease with which electric current flows between biosensors. Here, a single well is shown at two different time points (pre- and postCPE). Note that, for clarity, only two biosensors are shown in the well bottom, and neither the cells nor the biosensors are drawn to scale.

Reisen and colleagues evaluated the efficacy of xCELLigence RTCA for determining the titers of West Nile virus (WNV) and Louis encephalitis virus (SLEV). Vero cells in suspension were incubated with serial dilutions of a known concentration of WMV or SLEV for 30 minutes at 37 °C. This was followed by immediate addition of the cell/virus suspension to E-Plate wells and the subsequent monitoring of impedance in an xCELLigence instrument. In contrast with uninfected control cells, which grew to confluency and maintained a plateaued CI, virus-infected cells displayed a time-dependent decrease in CI down to zero, indicating complete cell lysis (Figures 12A and 12B). Consistent with the known cytolytic activities of WNV and SLEV, WNV displays both an earlier onset of CPE and a more rapid rate of CPE progression when monitored by xCELLigence.

Significantly, for both WNV and SLEV, the time at which the cytopathic effect occurred correlated extremely well with the known titer of the virus. This was highlighted by plotting the CIT50 (time required for the Cell Index to decrease by 50%) as a function of virus titer (lower panels of Figures 12A and 12B). Using this type of standard curve, it was possible to determine the viral titer in samples of unknown concentration. Beyond characterizing viral stocks being used for research purposes, this approach can be applied in the clinic to quantify the load of a specific virus in samples.
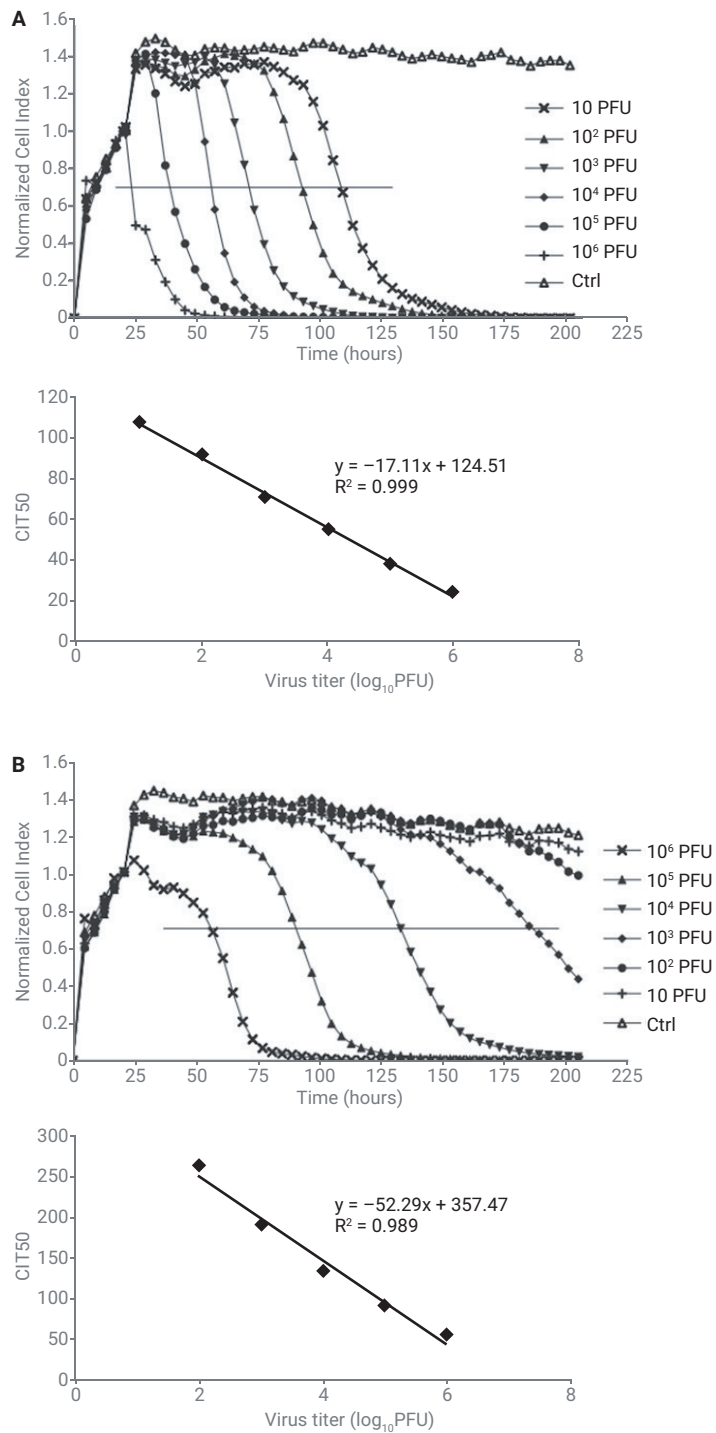
**Figure 12.** Using an Agilent xCELLigence RTCA instrument to determine viral titer. (A) Upper panel: real-time monitoring of WNV-induced cytopathic effect in Vero cells. The normalized CI is shown for E-Plate wells that were inoculated with a negative control (Ctrl) or different numbers of plaque forming units (PFU) of WNV. Each curve is an average of two independent replicate wells. The horizontal line denotes the point at which the CI has dropped to 50% of its initial value (that is, before virus addition). The time required to reach this point is referred to as CIT50. Lower panel: by plotting CIT50 as a function of viral titer, a standard curve was produced, which can be used for determining virus concentration in samples. (B) Real-time monitoring of SLEV-induced cytopathic effect in Vero cells. Experimental details and data processing are similar to part A.

Reprinted from the *Journal of Virological Methods*, volume *173 (2)*, Fang, Y. *et al.* "Real-time monitoring of flavivirus induced cytopathogenesis using cell electric impedance technology." Copyright **2011**, with permission from Elsevier.

References—RTCA for virus titer determination

1. Fang, Y. *et al.* Real-Time Monitoring of Flavivirus Induced Cytopathogenesis Using Cell Electric Impedance Technology. *J. Virol. Methods.* **2011** May, *173(2)*, 251–8.

2. Witkowski, P. T. *et al.* Cellular Impedance Measurement as a New Tool for Poxvirus Titration, Antibody Neutralization Testing and Evaluation of Antiviral Substances. *Biochem. Biophys. Res. Commun.* **2010** Oct 8, *401(1)*, 37–41.

3. Charretier, C. *et al.* Robust Real-Time Cell Analysis Method for Determining Viral Infectious Titers During Development of a Viral Vaccine Production Process. *J. Virol. Methods* **2017** Nov 14, *252*, 57–64.

4. Charretier, C. *et al.* Robust Real-Time Cell Analysis Method for Determining Viral Infectious Titers During Development of a Viral Vaccine Production Process. *J. Virol. Methods* **2018** Feb, *252*, 57–64 (republished).

5. Burmakina, G. *et al.* Real-Time Analysis of the Cytopathic Effect of African Swine Fever Virus. *J. Virol. Methods* **2018** Jul, *257*, 58–61.

6. Lebourgeois, S. *et al.* Development of a Real-Time Cell Analysis (RTCA) Method as a Fast and Accurate Method for Detecting Infectious Particles of the Adapted Strain of Hepatitis A Virus. *Front. Cell Infect. Microbiol*. **2018** Sep 25, *8*, 335.

# Viruses: neutralizing antibodies

The principles underlying the use of xCELLigence RTCA for monitoring virus-induced cytopathic effects (CPEs) are described in detail in the *Viruses: titer determination* chapter. This real-time viral CPE assay can be used for many applications, including the detection and quantification of neutralizing antibodies, as described below.

After growing Vero cells to confluence in E-Plate wells, Fang and coworkers infected each well with $10^6$ plaque-forming units of West Nile Virus (WNV) that had been pre-incubated with serially diluted neutralizing antibody of known concentration.[1] As shown in Figure 13A, the onset of WNV-induced CPE was delayed by the neutralizing antibody in a manner that was directly dependent on antibody concentration. By plotting the CIT50 (time required for the CI to decrease by 50%) as a function of the antibody titer, a standard curve was generated (Figure 13B), which could be used for quantifying the amount of neutralizing antibody present in avian specimens. Using this standard curve to determine antibody concentrations in infected birds out in the wild gave values that correlated very well with values determined by a traditional plaque-reduction neutralization test.[1]
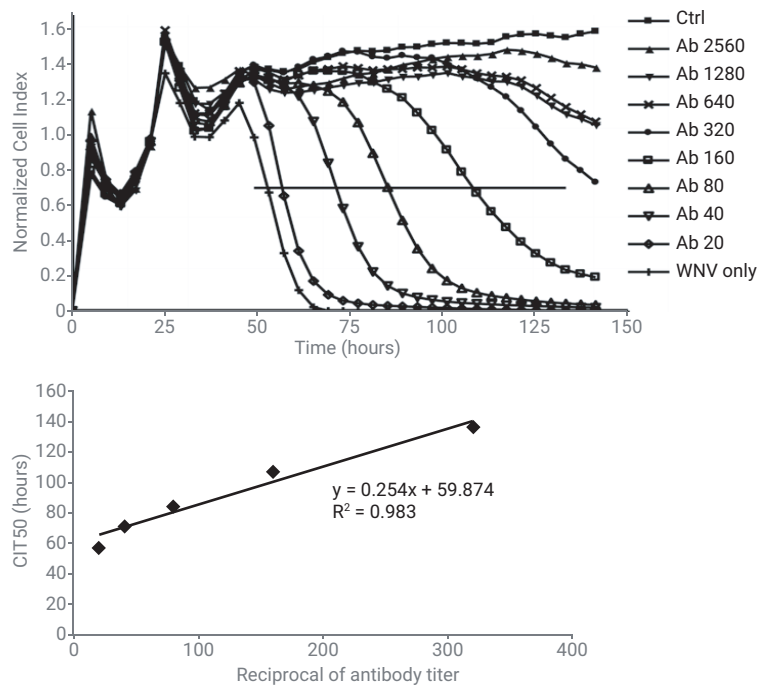
**Figure 13.** Quantifying WNV neutralizing antibody titer using an Agilent xCELLigence RTCA instrument. (A) Vero cells were infected with $10^6$ plaque-forming units of WNV that had been pre-incubated with different dilutions of neutralizing antibody. Ctrl = Vero cells that were not infected with virus; WNV only = Vero cells infected with virus that was not pre-exposed to antibody. The horizontal line denotes the point at which Cell Index has dropped to 50% of its initial value (that is, before virus addition). The time required to reach this point is referred to as CIT50. (B) By plotting CIT50 as a function of the reciprocal of antibody titer, a standard curve is produced which can be used for assessing the antibody concentrations in wild avian sera.

Reprinted from *Journal of Virological Methods*, volume *173 (2)*, 251–8, Fang, Y. *et al.* "Real-Time Monitoring of Flavivirus Induced Cytopathogenesis Using Cell Electric Impedance Technology." Copyright **2011**, with permission from Elsevier.

In a manner similar to that described above for WNV, RTCA has also been used for quantifying the amount of neutralizing antibody against the influenza A H1N1 virus present in human sera. In E-Plate wells, confluent cells were infected with purified H1N1 virus that either had or had not been pretreated with serum (Figure 14). The collection of the serum samples before vaccination, 7 days post vaccination, or 21 days post vaccination provided the possibility to track the emergence of an H1N1-specific neutralizing response over time. As expected, the robustness of the H1N1 neutralizing antibody activity increased progressively over the first 21 days postvaccination, evidenced by the delayed onset or complete block of the cytopathic effect.
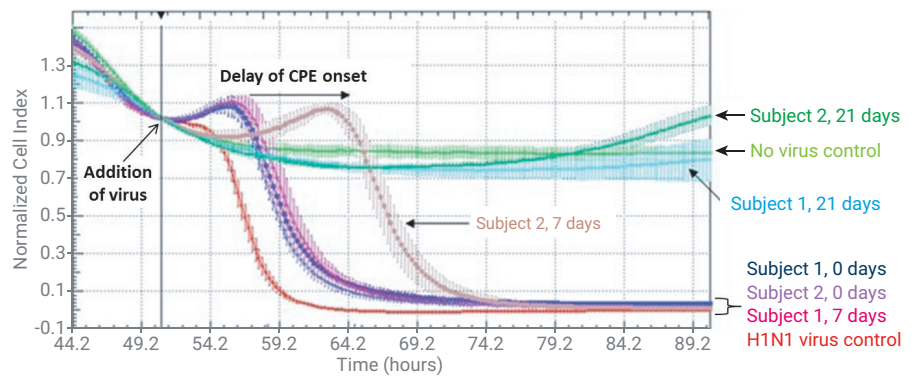
**Figure 14.** Measuring neutralizing antibody activity in H1N1-vaccinated subjects using RTCA to track delayed onset of cytopathic effect. Serum samples from two subjects were collected before vaccination (day 0), then 7 and 21 days postvaccination. These serum samples were incubated with purified H1N1 virus before adding the virus/serum mixture to cells growing in an Agilent E-Plate. For both subjects, serum from day 0 provides no protection, and the virus kills the cells with kinetics very similar to the positive control. For subject 2, serum from day 7 showed significant delay of H1N1-induced CPE, indicating the presence of specific neutralizing antibodies against H1N1 virus. In contrast, subject 1's serum at day 7 showed no prophylactic effect, indicating that an H1N1 neutralizing antibody activity was not yet present. However, 21 days postvaccination, the serum from both subjects displayed robust neutralizing antibody activity against H1N1, rendering the virus completely incapable of inducing a cytopathic effect. This assay makes it possible to quantitatively assess the efficacy of a particular vaccine, as well as the kinetics of virus resistance emergence.

Figure adapted from *Asia Pacific Biotech News*, volume *14 (10)*, Lu, H. *et al.* "Label-free Real-time Cell Based Assay System for Evaluating H1N1 Vaccination Success," pages 31–32. Copyright **2010**, with permission from Asia Pacific Biotech News.

With its simple, automated workflow and objective and quantitative readout, RTCA offers clear advantages over traditional assays for detecting and quantifying neutralizing antibodies. This approach provides a simple means for monitoring the efficacy of vaccination, and for elucidating the kinetics of virus resistance emergence.

## References—RTCA for studying neutralizing antibodies

1. Fang, Y. *et al.* Real-time Monitoring of Flavivirus Induced Cytopathogenesis Using Cell Electric Impedance Technology. *J. Virol. Methods*. **2011** May, *173(2)*, 251–8.

2. Lu, H.; Xu, X. Label-Free Real-Time Cell Based Assay System for Evaluating H1N1 Vaccination Success. *Asiabiotech.* **2010**, *14(10)*, 31–32.

3. Teng, Z. *et al.* Real-Time Cell Analysis—A New Method For Dynamic, Quantitative Measurement of Infectious Viruses and Antiserum Neutralizing Activity. *J. Virol. Methods.* **2013** Nov, *193(2)*, 364–70.

4. Burmakina, G. *et al.* Real-Time Analysis of the Cytopathic Effect of African Swine Fever Virus. *J. Virol. Methods* **2018** Jul, *257*, 58–61.

5. Tian, D. *et al.* Novel, Real-Time Cell Analysis for Measuring Viral Cytopathogenesis and the Efficacy of Neutralizing Antibodies to the 2009 Influenza A (H1N1) virus. *PLoS One* **2012**, *7(2)*, e31965.

# Viruses: drug screening

Real-time impedance monitoring is sensitive to virus-induced cytopathic effects, making xCELLigence an excellent tool for identifying and characterizing drugs that inhibit any facet of the virus lifecycle.

Urs Greber and colleagues at the Institute of Molecular Life Sciences in Zurich aimed to identify a drug that could mitigate the effects of adenovirus in subjects already infected with the virus. Their screening assay involved growing HeLa cells to confluence, then infecting them with human adenovirus in the presence of different drug candidates. Most effective among these was flavopiridol, a semisynthetic flavonoid compound known to inhibit the cell cycle-dependent kinase Cdk9. As shown in Figure 15A, in the absence of a drug, adenovirus infection induced a robust CPE with the impedance signal decreasing to zero (red trace). However, in a dose-dependent manner flavopiridol was able to significantly delay the onset of CPE (blue and orange traces). These findings based on impedance were corroborated by microscopy analysis (Figure 15B).
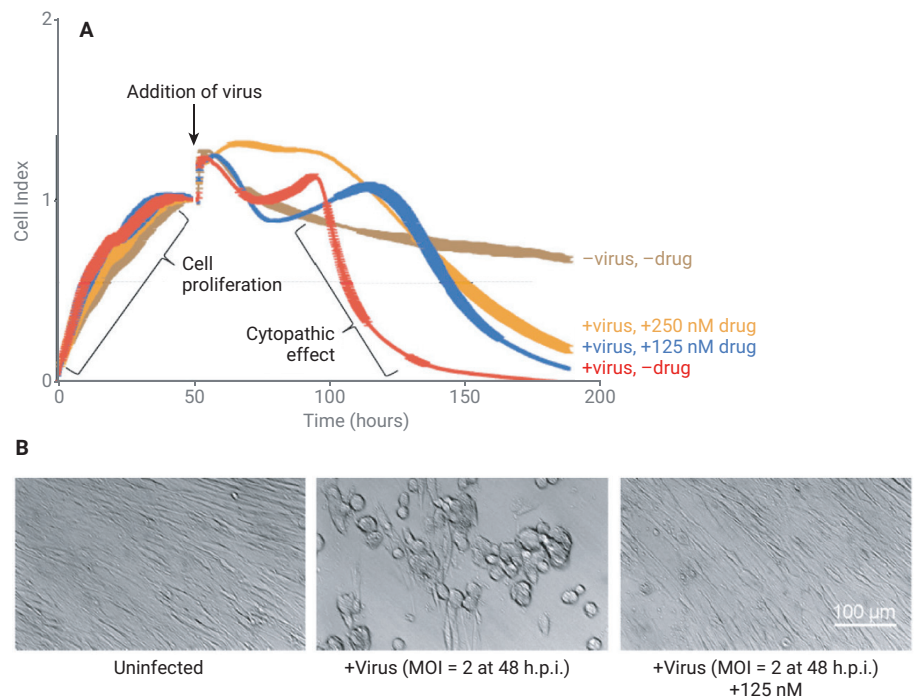


**Figure 15.** Monitoring antiviral activity of flavopiridol. (A) HeLa cells were grown in an Agilent E-Plate to the point of confluence. Roughly 50 hours postseeding, cells were infected with human adenovirus strain C5 in the presence of different concentrations of flavopiridol. (B) Flavopiridol affords broad protection against adenovirus. Here, WI38 lung fibroblasts were infected with human adenovirus strain D37, and four hours later flavopiridol either was or was not added. At 48 hours postinfection, the drug is clearly seen to have prevented a cytopathic effect from occurring.

Figure adapted with permission from *ACS Infectious Diseases* Volume *3 (6)*, Prasad, V. *et al.* "Cell Cycle-Dependent Kinase Cdk9 Is a Postexposure Drug Target Against Human Adenoviruses," pages 398–405. Copyright **2017**, American Chemical Society

In a second example, Guy Boivin and coworkers at Laval University in Quebec analyzed the sensitivity of WT and mutant herpes simplex virus 1 (HSV-1) to the antiviral acyclovir. After being grown to confluence in E-Plates, Vero cells were infected with the virus for 90 minutes before adding different concentrations of the drug. Although the CPE induced by both WT and mutant virus could be blocked by acyclovir, a much higher concentration of the drug was required for blocking the mutant strain than the WT strain (Figure 16). By plotting the CI value at a given time point as a function of drug concentration, dose response curves were generated (data not shown here), yielding EC50 values of 100 µm and 0.8 µM for the mutant and WT viruses, respectively. These findings were consistent with this particular mutant strain of the virus having a mutation in its DNA polymerase, which is the target of acyclovir.
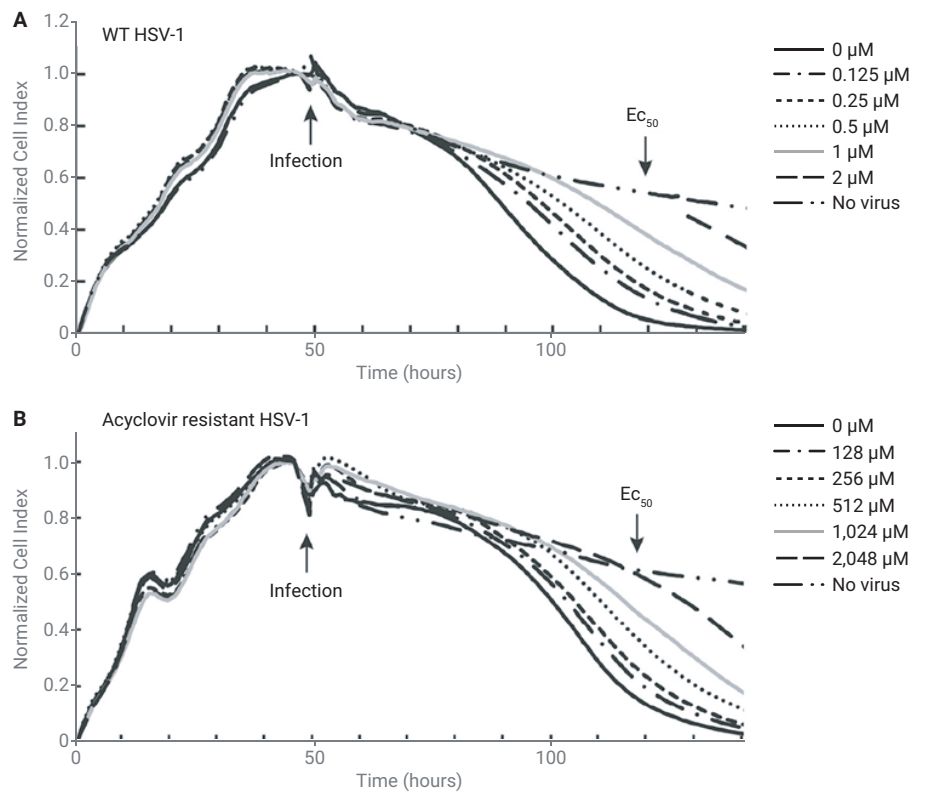


**Figure 16.** Comparing acyclovir sensitivity of WT and mutant HSV-1. Vero cells were grown to confluence in an Agilent E-Plate. Forty-eight hours postseeding, cells were infected with either WT or mutant HSV-1 for 90 minutes. Different concentrations of acyclovir were then added, and impedance was monitored every 30 minutes for an additional 100 hours. Note that much higher concentrations of the drug were required to prevent the cytopathic effect for the mutant.

Data adapted from the *Journal of Clinical Microbiology*, volume *54 (8)*, Piret, J. *et al.* "Novel Method Based on Real-Time Cell Analysis for Drug Susceptibility Testing of Herpes Simplex Virus and Human Cytomegalovirus." Copyright **2016**, with permission from American Society for Microbiology.
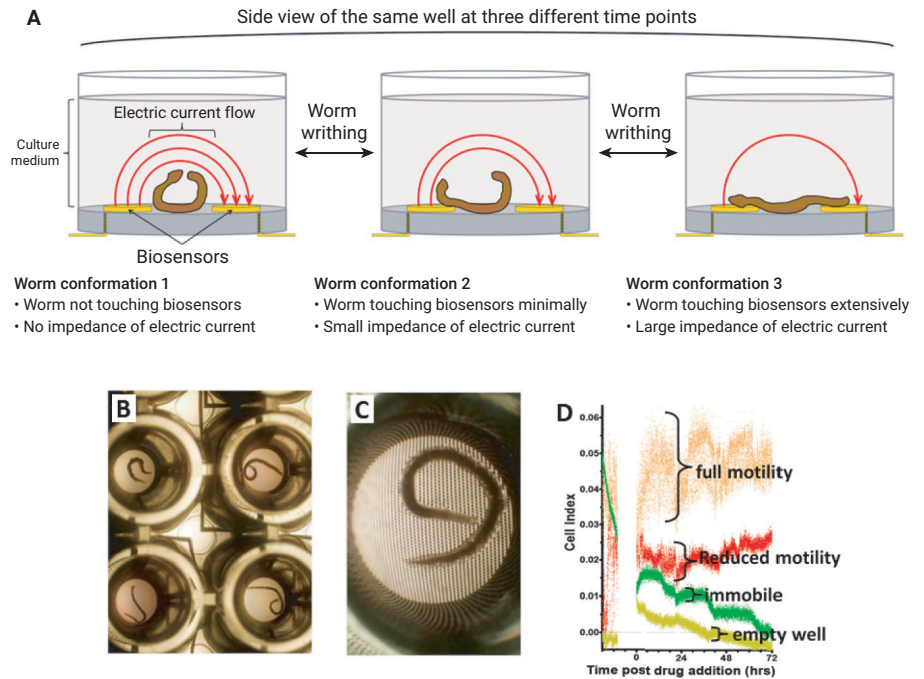
References—RTCA for viral drug screening

1. Watterson, D. *et al.* A Generic Screening Platform for Inhibitors of Virus Induced Cell Fusion Using Cellular Electrical Impedance. *Sci. Rep.* **2016** Mar 15, *6*, 22791.

2. Zandi, K. A Real-Time Cell Analyzing Assay for Identification of Novel Antiviral Compounds against Chikungunya Virus. *Methods Mol. Biol.* **2016**, *1426*, 255–62.

3. Sharma, B. N. *et al.* Antiviral Effects of Artesunate on Polyomavirus BK Replication in Primary Human Kidney Cell. *Antimicrob. Agents Chemother.* **2014**, *58(1)*, 279–89.

4. Witkowski, P. T. *et al.* Cellular Impedance Measurement as a New Tool for Poxvirus Titration, Antibody Neutralization Testing and Evaluation of Antiviral Substances. *Biochem. Biophys. Res. Commun.* **2010** Oct 8, *401(1)*, 37–41.

5. Piret, J. *et al.* Novel Method Based on Real-Time Cell Analysis for Drug Susceptibility Testing of Herpes Simplex Virus and Human Cytomegalovirus. *J. Clin. Microbiol.* **2016** Aug, *54(8)*, 2120–7.

6. Cymerys, J. *et al.* Primary Cultures of Murine Neurons for Studying Herpes Simplex Virus 1 Infection and Its Inhibition by Antivirals. *Acta Virol.* **2013**, *57(3)*, 339–45.

7. Prasad, V. *et al.* Cell Cycle-Dependent Kinase Cdk9 Is a Postexposure Drug Target Against Human Adenoviruses. *ACS Infect. Dis.* **2017** Jun 9, *3(6)*, 398–405.

# Parasitic worms

Living within the intestines or blood vessels of their hosts, parasitic worms (helminths) inhabit more than one billion people globally, and cause hundreds of thousands of deaths annually. Despite the prevalence and expense of helminth infection, the helminth-specific pharmacopeia is extremely limited. This is historically due, in part, to the paucity of objective high-throughput drug screening methods amenable to the life cycle of these parasites. For many years, the primary screening tool has been manual monitoring of the rate at which the worms move/writhe when viewed under a microscope.

With the goal of developing a high-throughput anthelmintic drug screening methodology, Smout and colleagues demonstrated that real-time impedance monitoring with xCELLigence RTCA is able to quantify parasitic worm motility (which is a surrogate of viability).[1] When a parasitic worm was placed within an E-Plate well, its movement changed the electrode surface area being contacted (Figures 17A to 17C), and consequently, the impedance signal fluctuated (Figure 17D). Whereas rapid temporal fluctuation of CI over a broad range of magnitudes was indicative of a fully active worm, slower temporal fluctuation over a narrow range of CI values was indicative of a lethargic/sick/dying worm (Figure 17D). In these types of plots, to make the data easier to read, the impedance trace for each condition was spread out on the Y-axis to prevent them from overlapping. The absolute value of the CI is not important; what is being compared among the different conditions was the rate and magnitude of CI fluctuation (Figure 17D).

**A** Side view of the same well at three different time points

**Worm conformation 1**
• Worm not touching biosensors
• No impedance of electric current

**Worm conformation 2**
• Worm touching biosensors minimally
• Small impedance of electric current

**Worm conformation 3**
• Worm touching biosensors extensively
• Large impedance of electric current

**Figure 17.** Using RTCA to screen for anthelmintic drugs. (A) As a worm writhes within an Agilent E-Plate well, the total electrode surface area that the worm is in contact with changes constantly, thereby causing the impedance signal to fluctuate. (B) Micrograph of adult *Ancylostoma caninum* hookworms inside E-Plate wells; females are shown in the top two wells, males are shown in the bottom two wells. (C) Zoomed view of an adult female *Ancylostoma caninum* laying on top of the electrode grid in a well. (D) Example data showing distinct impedance traces for healthy versus drug-impaired worms. **Note:** the numerical value of the Cell Index is not relevant to this analysis. The curves have been manually repositioned along the Y-axis to assist with visualization of the data (that is, to prevent the four curves from overlapping with one another). The rate at which the CI fluctuates, and the magnitude of its fluctuation are the critical parameters here. See text for details.

Figure adapted from *Public Library of Science Neglected Tropical Diseases*, volume *4 (11)*, Smout, M. J. *et al.* "Novel High Throughput Assay for Anthelmintic Drug Screening and Resistance Diagnosis by Real-Time Monitoring of Parasite Motility " **2010**.

Using impedance monitoring, Smout and coworkers were able to screen for drug efficacy against three different stages of the parasitic worm life cycle. Figures 18A and 18B highlight where levamisole and thiabendazole were shown to effect the L3 larval stage and the egg hatching stage of *Haemonchus contortus*, respectively. In a standard worm motility assay, L3 larvae were lethargic at a levamisole concentration of 0.4 µg/mL, but were killed when the concentration was raised to 6 µg/mL (Figure 18A). To evaluate the effect of thiabendazole on egg hatching, eggs were placed on top of a mesh screen positioned above E-Plate biosensors. As eggs hatched and the larvae crawled through the screen they came into contact with the E-Plate biosensors, and caused the impedance signal to increase in a manner that was proportional to the total number of hatched eggs. Thiabendazole was found to suppress this egg hatching process in a dose-dependent manner (Figure 18B).

These findings are particularly important as they demonstrate that RTCA can be used to cast a very broad net during anthelmintic drug screening: as each stage in a parasitic worm's life cycle may display differential drugability, being able to monitor three of them increases the chances of success.
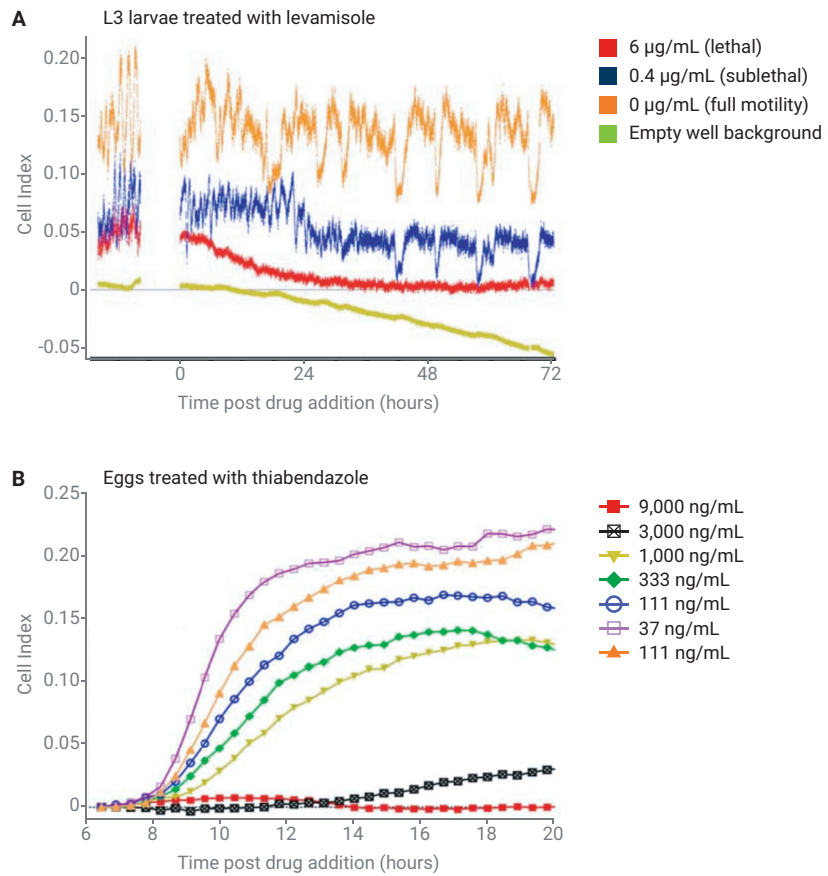


**Figure 18.** Identifying drugs that are effective against different stages of the *H. contortus* life cycle. (A) Levasmisole is effective against the L3 larval stage. Whereas a concentration of 0.4 µg/mL slightly reduced larval motility, a concentration of 6 µg/mL was lethal. Note: the numerical value of the Cell Index is not relevant to this analysis; the curves have been manually repositioned along the Y-axis to assist with visualization of the data (that is, to prevent the four curves from overlapping with one another). The rate at which the CI fluctuates, and the magnitude of its fluctuation are the critical parameters here. (B) Egg hatching in the presence of varying amounts of the drug thiabendazole. Note that increasing drug concentrations result in less egg hatching and a smaller impedance signal. See text for details.

Figure adapted from *Public Library of Science Neglected Tropical Diseases*, volume *4 (11)*, Smout, M. J. *et al.* "A Novel High Throughput Assay for Anthelmintic Drug Screening and Resistance Diagnosis by Real-Time Monitoring of Parasite Motility " 2010.

## References—RTCA for studying parasitic worms

1. Smout, M. J. *et al.* A Novel High Throughput Assay for Anthelmintic Drug Screening and Resistance Diagnosis by Real-Time Monitoring of Parasite Motility. *PLoS Negl. Trop. Dis.* **2010** Nov 16, *4(11)*, e885.

2. Rinaldi, G. *et al.* Viability of Developmental Stages of *Schistosoma mansoni* Quantified with xCELLigence Worm Real-Time Motility Assay (xWORM). *Int. J. Parasitol. Drugs Drug Resist.* **2015** Aug 6, *5(3)*, 141–8.

3. Zeraik, A. E. *et al.* Reversible Paralysis of *Schistosoma mansoni* by Forchlorfenuron, a Phenylurea Cytokinin that Affects Septins. *Int. J. Parasitol.* **2014** Jul, *44(8)*, 523–31.

4. Hong, Y. *et al.* Transcriptional Responses of *In Vivo* Praziquantel Exposure in Schistosomes Identifies a Functional Role for Calcium Signaling Pathway Member CamKII. *PLoS Pathog.* **2013** Mar, *9(3)*, e1003254.

5. Silbereisen, A. *et al.* Exploration of Novel *In Vitro* Assays to Study Drugs Against *Trichuris* spp. *J. Microbiol. Methods.* **2011** Nov, *87(2)*, 169–75.

6. Tritten, L. *et al.* Comparison of Novel and Existing Tools for Studying Drug Sensitivity Against the Hookworm *Ancylostoma ceylanicum In Vitro*. *Parasitology* **2012** Mar, *139(3)*, 348–57.